CRYSTAL GROWTH & DESIGN

Communication

pubs.acs.org/crystal

Organized Surfaces of Highly Faceted Single-Crystal Palladium Structures Seeded by Sacrificial Templates

Aarthi Sundar,[†] Pouyan Farzinpour,[†] Kyle D. Gilroy,[†] Teng Tan,[‡] Robert A. Hughes,[†] and Svetlana Neretina*[,†]

[†]College of Engineering, Temple University, Philadelphia, Pennsylvania 19122, United States

[‡]Department of Physics, Temple University, Philadelphia, Pennsylvania 19122, United States

ABSTRACT: The templated synthesis of periodic arrays of highly faceted single-crystal structures of palladium is described. The devised route confines an array of sacrificial gold templates between a palladium foil and a single-crystal oxide substrate. At elevated temperatures, the gold templates are annihilated and replaced with palladium structures situated at the precise locations formerly occupied by gold. The assembly process relies on the concurrent sublimation of palladium and gold, which results in the complete transfer of the templated gold from the substrate to the foil but not before the templates act as heterogeneous nucleation sites for palladium adatoms arriving to the substrate surface. The so-formed palladium structures take on the equilibrium Wulff shape expected for elements with a face-centered cubic crystal structure, where the shape and crystallographic alignment of the arrayed structures is promoted through a heteroepitaxial relationship with the underlying substrate. The assembled structures provide an excellent platform for advancing applications reliant on the unique hydrogen storage, catalytic, and plasmonic properties of palladium.

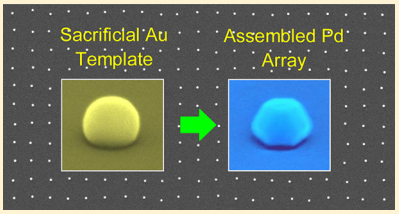

The templated synthesis of metallic structures provides the means by which assembly processes can be guided toward predetermined end points.[1] The role of the template is to exert control over such factors as the placement, shape, crystallography, and chemical composition of the assembling structure. Such templates can be chemically active in the assembly process or merely act as scaffolds upon which emerging structures adhere. In the former case, the template can become a part of the emerging structure or be consumed through destructive chemical transformations. Solution dispersed templates have yielded a myriad of structures with complex geometries exhibiting properties suitable for such applications as biological and chemical sensing,[2] catalysis,[3] and drug delivery.[4] The use of substrate-based templates, while less developed, also offers the potential for fabricating structures for plasmonic,[5] catalytic,[6] photovoltaic,[7] and detector applications.[8,9] Of significance to many of these applications is the establishment of templated routes where structures of the same size are assembled at prescribed locations such that there exists crystallographic and shape alignment relative to the underlying substrate.

Numerous modalities have been devised which use substrate-based templates to direct the assembly of metal structures. A substrate surface texture, for example, can act as a physical template which allows metal structures to assemble within pores exhibiting a well-defined geometry, the most common of which is anodic aluminum oxide (AAO) membranes.[10] A second approach takes advantage of the variation in curvature resulting from a substrate surface topography to direct the high temperature agglomeration of ultrathin metal films to precise locations.[11,12] The textures required for these two methods can, however, be disadvantageous from the standpoint of incorporating the assembled structures into device architectures. Templates formed directly on planar substrates provide a far more versatile platform for assembly processes, both in terms of the template makeup and its accessibility to the postassembly routes required for device fabrication. Notable examples include the (i) use of nanowires as scaffolds for nanoparticles with catalytic[13] or photoelectrochemical properties,[14] (ii) growth of nanowires from seeds which direct the assembly process,[15] and (iii) formation of hollow nanoshells through galvanic replacement reactions performed on sacrificial silver templates.[16,17]

In a previous report, we demonstrated a straightforward processing route capable of reducing the size of arrayed gold structures from submicrometer to nanoscale dimensions.[18] The route took advantage of the fact that the confinement of gold structures between a platinum foil and the oxide substrate upon which they were formed would, at elevated temperatures, result in a net migration of gold atoms from the substrate to the foil. In the report, we noted the possibility of not only sinking material to a confining foil but also sourcing it through the sublimation of atoms from the surface of the foil. Here, we report on the confinement of periodic arrays of gold structures between a palladium foil and a sapphire substrate. Observed is a templated assembly process which sees the gold structures act as sacrificial templates which are annihilated and replaced by organized surfaces of highly faceted structures of palladium.

Figure 1 shows a schematic of the devised templated assembly route. Periodic arrays of sacrificial gold templates (Figure 1a) were fabricated using dynamic templating, a

Received: June 28, 2013
Revised: August 2, 2013
Published: August 7, 2013

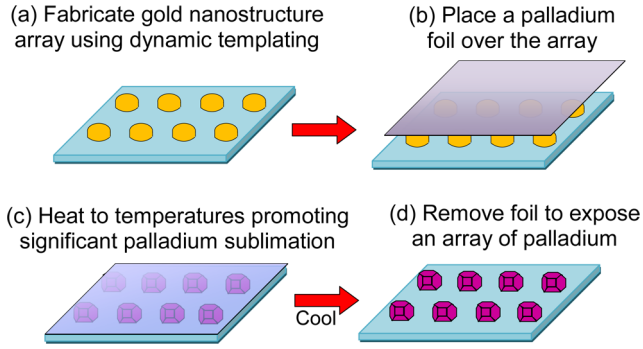

Figure 1. Schematic of the templated assembly process used to transform a periodic array of sacrificial gold templates into an array of palladium nanostructures. The process involves (a) the fabrication of a gold array, followed by (b) placing a palladium foil over the array and (c) heating the combination to 1085 °C. This temperature is high enough to promote palladium sublimation from the foil to the substrate and the complete evaporation of the gold template onto the foil. At the end of the assembly process, the foil is removed to reveal (d) a periodic array of highly faceted palladium nanostructures situated at the positions formerly occupied by the sacrificial gold templates.

lithography-free processing route which we describe in detail elsewhere.[19] Briefly, bismuth/antimony pedestals (40 nm Sb and 10 nm Bi) topped with a thin layer of gold are sputter deposited through shadow masks (900 nm diameter openings, center-to-center distance of 1.6 μm). When exposed to elevated temperatures, pedestal annihilation through evaporation/sublimation causes a forced agglomeration of gold to the center of each pedestal, a process which results in the formation of a periodic array of gold nanostructures. A gold layer thickness of 10 nm yielded structures with a diameter of 230 nm. The heating regimen used to form these arrays involved twice heating the sample from room temperature to 1050 °C in 20 min in a flowing argon ambient (65 sccm) followed by a 3 h cool down to room temperature. Palladium foil (0.025 mm thick, 99.9% purity) was then placed over the arrayed structures (Figure 1b), and the combination was placed into an alumina crucible and heated from room temperature to 1085 °C in 60 min, where it was held for time intervals ranging from 45 min to 10 h (Figure 1c). This temperature is sufficiently high to promote both palladium sublimation from the foil and gold evaporation from the nanoparticle. Subsequent cooling to room temperature over a period of 3 h followed by foil removal (Figure 1d) reveals the complete loss of gold to the foil and the existence of highly faceted palladium nanostructures at the exact positions previously occupied by the gold structures. The assembly process was carried out using either [0001]-oriented Al_2O_3 (i.e., c-plane sapphire) or [111]-oriented MgO substrates.

Figure 2 shows scanning electron microscopy (SEM) images taken in a secondary electron mode and the corresponding energy-dispersive X-ray spectroscopy (EDS) peaks for both the sacrificial gold templates and the assembled palladium structures. The arrayed gold templates (Figure 2a) exhibit a near-hemispherical morphology (dia. = 230 nm), but where weak faceting is observed. As expected, the corresponding EDS spectrum shows peaks characteristic of gold. After assembly, the palladium structures become highly faceted (Figure 2b) exhibiting facets approaching that of the substrate-truncated Wulff shape (i.e., a truncated octahedron enclosed by eight {111} facets and six {100} facets, which is further truncated by approximately 25% at the substrate−nanostructure interface due to surface energy considerations) expected for face centered cubic (fcc) crystal structures.[20] The fact that the facets on adjacent structures are, for the most part, parallel to each other confirms the existence of a predominant heteroepitaxial relationship between the structures and the underlying crystalline substrate. The structures, which are 220 nm in diameter, show EDS peaks corresponding only to palladium, a clear indication that gold is consumed during the assembly process. Assembly processes carried out for shorter time intervals do, however, show residual levels of gold. Also noteworthy is that palladium sublimation onto the sapphire surface for these long durations does not result in the nucleation of nanostructures in the areas between the arrayed structures. Long duration experiments were carried out to determine if the palladium structures (i) grow in size, (ii) diminish in size, or (iii) assume a size corresponding to a steady-state condition. These experiments revealed a slowly

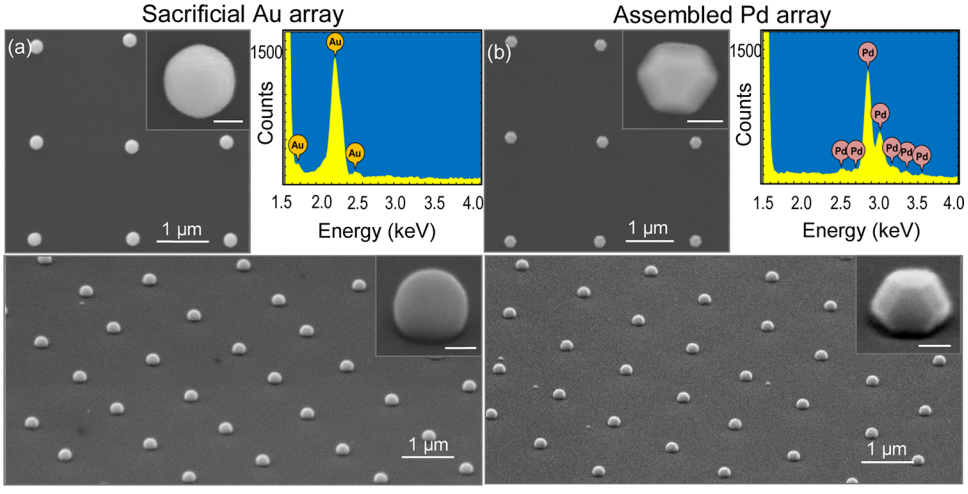

Figure 2. SEM images and the associated EDS spectra of (a) sacrificial gold templates and (b) the highly faceted palladium structures obtained after the completion of the templated assembly process. Note that peaks corresponding to gold are absent in the EDS spectrum of the assembled palladium structures. The insets to the SEM images show 65° tilted- and top-view high-resolution images of individual structures. The scale bar for the insets is 100 nm.

dx.doi.org/10.1021/cg400974f | *Cryst. Growth Des.* 2013, 13, 3847−3851

diminishing diameter that leaves the substrate bare after 6 h. These long time intervals allow for precise control over the size of the palladium nanostructures realized in the assembly process. The smallest arrayed palladium nanostructures produced to date have a diameter of 50 nm.

θ–2θ X-ray diffraction (XRD), a technique sensitive to periodicities perpendicular to the surface of the substrate, was used to confirm the gold to palladium transformation and to determine the crystallographic orientation of the structures with respect to the underlying substrate. The relatively small amount of material in the arrayed structures required that these measurements be carried out on nonarrayed structures produced over much larger areas. The so-formed structures appear identical to the arrayed structures, but where there exists a substantial size distribution. The XRD data indicates that the gold templates are [111]-oriented (Figure 3a), a result

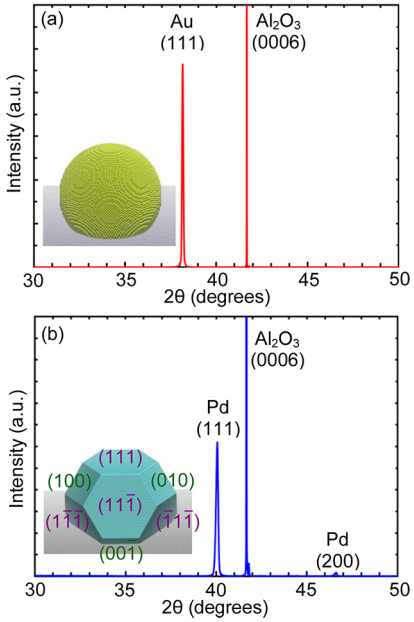

Figure 3. θ–2θ XRD scans performed on (a) sacrificial gold templates formed on [0001]-oriented sapphire and (b) the palladium structures formed in the assembly process. The assembly process results in the elimination of the (111) Au reflection and the emergence of a strong (111) Pd reflection. Both scans originate from the same sample. The insets to the figures show schematics of the structures where the [111]-oriented palladium structure has its facets labeled.

consistent with a heteroepitaxial relationship formed between the (0001)-plane of sapphire and the 6-fold symmetric (111)-plane of the fcc crystal structure of gold. Following the assembly process, there is no gold signature in the X-ray data (Figure 3b). Instead, two reflections appear at the precise 2θ values associated with [111]- and [200]-oriented palladium, but where the [111]-orientation is dominant. The inset to Figure 3b shows a schematic of a [111]-oriented palladium structure with facet assignments consistent with the substrate truncated Wulff shape. On the basis of this X-ray data and the observed palladium nanostructure faceting relative to the substrate alignment flat, two dominant crystallographic orientation relationships (ORs) emerge: $(111)[\bar{2}11]_{Pd}\|(0001)[11\bar{2}0]_{sapphire}$ and $(111)[2\bar{1}\bar{1}]_{Pd}\|(0001)[11\bar{2}0]_{sapphire}$. It should be noted that both these ORs are also observed for twinned fcc copper films deposited on (0001)-oriented sapphire.[21] The two orientations differ in that one has an ABC stacking sequence along the [111]-direction, while the other exhibits a CBA sequence.

Individual gold and palladium structures were characterized using transmission electron microscopy (TEM). For these studies, samples were prepared on [111]-oriented MgO substrates instead of sapphire through the thermal dewetting of thin gold films.[22] The [111]-oriented palladium nanostructures prepared on MgO appear identical to those on sapphire in terms of morphology, composition, and crystal structure. There, however, exists a significant number of structures with [100]- and [110]-orientations due to the large lattice mismatch (8%). The structures were prepared on MgO in order to facilitate their removal from the substrate. The removal process took advantage of the fact that dilute hydrochloric acid (0.5%) selectively etches the substrate. Once the etchant undercuts the structures, they were readily removed and collected on a TEM grid. TEM images and their corresponding selected area electron diffraction (SAED) patterns are shown in Figure 4 for a gold template and for palladium structures imaged along various zone axes. As expected, the gold templates show weak faceting. The palladium structures exhibit single-crystal SAED patterns with strong faceting. For all three cases the imaged faceting corresponds to a projection of the Wulff shape oriented along the same zone axis, as is shown schematically in Figures 4 (panels b–d).

This initial investigation demonstrates the utility of using substrate-based sacrificial templates to define site-specific locations which promote the assembly of highly faceted and heteroepitaxially aligned single-crystal palladium nanostructures. The devised route is straightforward in that sacrificial templates are merely exposed to a palladium foil which, at the processing temperatures used, acts as both a source and a sink for atoms involved in the assembly process. Insights into the mechanisms guiding this process are most readily obtained by first examining the experimental outcomes when key elements of the assembly process are absent. In the first scenario, the gold templates are removed from the assembly process, resulting in a bare sapphire substrate being exposed to palladium foil. Under identical experimental conditions as the devised assembly process, no palladium nanostructures are formed on the sapphire substrate despite the fact that palladium is slowly sublimating onto its surface. This is due to the fact that the palladium adatoms diffusing along the substrate are insufficient in number to nucleate stable clusters. Adatoms traveling along the surface will eventually acquire the thermal activation energy required to leave the surface and return to the foil. The system is, thus, characterized by a steady-state condition where palladium atoms are traveling back and forth between the foil and substrate but where no nanostructures of significance are formed. It is, however, noted that Ma et al.[23] have demonstrated that nanostructure formation becomes viable at significantly higher temperatures where the palladium flux arriving to the substrate is much greater. In the second scenario, gold templates are heated to the assembly temperature in the absence of palladium foil. As the templates are heated, they begin to lose material, first through sublimation and then via evaporation once the gold melting point (T_m = 1064 °C) has been exceeded. Eventually, all the template material leaves the surface and is carried away by the flowing argon gas or deposited on the sidewalls of the quartz reaction tube. It should be noted that the rate at which template material is lost is dependent on such factors as the temperature, the size, and curvature of the nanostructure (i.e., the Gibbs–Thomson

dx.doi.org/10.1021/cg400974f | Cryst. Growth Des. 2013, 13, 3847–3851

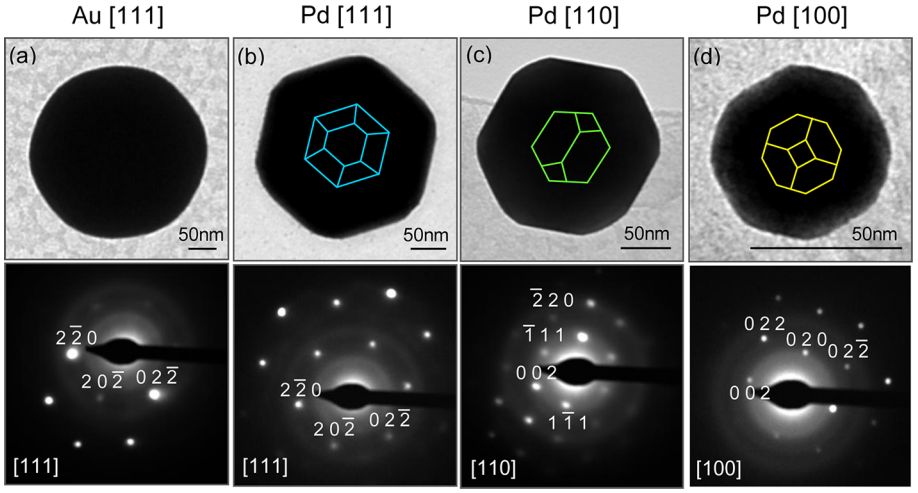

Figure 4. TEM images and the corresponding SAED pattern of (a) a sacrificial gold template formed on [111]-oriented MgO and palladium structures imaged along (b) [111], (c) [110], and (d) [100] zone axes. Overlaid on each palladium image is a schematic of the projection of the Wulff shape of the same orientation.

effect) and the argon gas pressure.[24] With both of these scenarios giving rise to bare substrates, it is apparent that the viability of the devised assembly process is dependent upon an interplay between the palladium adatoms arriving from the foil and the rapidly evaporating gold templates.

The early stages of the assembly process are characterized by the onset of gold evaporation and the concurrent sublimation of palladium from the foil. At the assembly temperature, the bulk vapor pressure of gold is approximately three times that of palladium. Thus, the molten gold droplet, although rapidly diminishing in size, is impinged by palladium adatoms both directly and via surface diffusion. The droplet not only provides a high surface energy nucleation site to the palladium but also offers complete miscibility, a property which in combination with the high processing temperatures further ensures palladium uptake into the structure. As the palladium concentration increases, the structure progresses from the liquid to solid phase fields of the binary phase diagram. At the assembly temperature, the solidus for the bulk material is intercepted at a palladium concentration of 12 atomic %. The second stage of the assembly process sees the palladium concentration in the structure continue to increase. The significant vapor pressure for both gold and palladium will inevitably result in their sublimation from the structure, where palladium is continuously replenished by the constant arrival of new adatoms. Gold atoms leaving the structure, on the other hand, are unlikely to return. If they land on the palladium foil, they can diffuse into its surface either via vacancy diffusion or along grain boundaries. Even if the gold does return to the substrate, its lifetime on the surface is considerably lower than palladium due to its higher vapor pressure, lowering the likelihood that it will encounter an arrayed structure. With the gold content in the structure being exhausted and the palladium supply essentially inexhaustible, the structure, as a function of time, trends toward pure palladium. The overall assembly process can, thus, be characterized as one where gold templates act as heterogeneous nucleation sites, where they are subsequently consumed through evaporative and sublimative processes. It should be noted that the palladium structures are metastable at the assembly temperature as is apparent by a steadily diminishing diameter occurring over long time intervals and which culminates in the complete annihilation of the structure.

While the shape and crystallographic control of substrate-based palladium nanostructures have been demonstrated previously,[25] the devised templated assembly route offers further opportunities in terms of defining such structures in periodic arrays with a high degree of size uniformity. Such a capability provides the potential for advancing applications based on the unique hydrogen storage,[26] plasmonic,[27] and catalytic properties of palladium.[28] Sensing applications reliant on an altered plasmonic response due to hydrogen uptake have shown impressive sensitivity.[29,30] Large area arrays of identical nanostructures also provide an excellent platform for obtaining a quantitative assessment of the facet dependent nature of the catalytic activity and selectivity of nanostructures.[9] These palladium structures could also act as nucleation sites for the formation of horizontally and vertically aligned palladium nanowires,[15,31,32] arrayed seeds for the vapor−liquid−solid growth of nanowires,[21,33,34] or templates for substrate-based galvanic replacement reactions.[16] The growth pathway can also be readily extended to other material systems. The use of cobalt and nickel foils instead of palladium has already yielded similar results. The growth pathway could also be adapted through the use of templates, which are not sacrificed in the assembly process. In this scenario, they would first act as heterogeneous nucleation sites but then evolve to form alloys with the material being sourced from the adjacent surface. The formation of eutectic combinations which subsequently phase separate upon cooling also provide the opportunity for forming substrate-based nanoheterostructures.

To summarize, we have devised a templated assembly route yielding periodic arrays of highly faceted single-crystal palladium structures from sacrificial gold templates. The high temperature processing route sees the continuous arrival of palladium atoms to the substrate surface, but where structure formation is energetically favorable only at the heterogeneous nucleation sites temporarily provided by sacrificial gold templates. The arrayed nature and narrow size distribution of the assembled structures provide an excellent platform for advancing applications and assembly processes reliant on the unique properties of palladium.

AUTHOR INFORMATION

Corresponding Author

*E-mail: neretina@temple.edu.

Notes

The authors declare no competing financial interest.

ACKNOWLEDGMENTS

This work is funded by the NSF CAREER Award of SN (DMR-1053416). The authors acknowledge the expertise of Dr. F. Monson (Technical Director, Center for Microanalysis, Imaging, Research and Training, West Chester University). The work has benefitted from the facilities available through Temple University's Material Research Facility (MRF) and University of Pennsylvania's Nanoscale Characterization Facility. K.D.G. acknowledges support received through a Temple University Graduate Student Fellowship.

REFERENCES

(1) Jones, M. R.; Osberg, K. D.; Macfarlane, R. J.; Langille, M. R.; Mirkin, C. A. *Chem. Rev.* **2011**, *111*, 3736−3827.

(2) Jans, H.; Huo, Q. *Chem. Soc. Rev.* **2012**, *41*, 2849−2866.

(3) Herves, P.; Perez-Lorenzo, M.; Lis-Marzan, L. M.; Dzubiella, J.; Lu, Y.; Ballauff, M. *Chem. Soc. Rev.* **2012**, *41*, 5577−5587.

(4) Yavuz, M. S.; Cheng, Y.; Chen, J.; Cobley, C. M.; Zhang, Q.; Rycenga, M.; Xie, J.; Kim, C.; Song, K. H.; Schwartz, A. G.; Wang, L. V.; Xia, Y. *Nat. Mater.* **2009**, *8*, 935−939.

(5) Schuller, J. A.; Barnard, E. S.; Cai, W.; Jun, Y. C.; White, J. S.; Brongersma, M. L. *Nat. Mater.* **2010**, *9*, 193−204.

(6) Stratakis, M.; Garcia, H. *Chem. Rev.* **2012**, *112*, 4469−4506.

(7) Atwater, H. A.; Polman, A. *Nat. Mater.* **2010**, *9*, 205−213.

(8) Shegai, T.; Johansson, P.; Langhammer, C.; Käll, M. *Nano Lett.* **2012**, *12*, 2464−2469.

(9) Liu, N.; Tang, M. L.; Hentschel, M.; Giessen, H.; Alivisatos, A. P. *Nat. Mater.* **2011**, *10*, 631−636.

(10) Yao, J.; Liu, Z.; Liu, Y.; Wang, Y.; Sun, C.; Bartal, G.; Stacy, A. M.; Zhang, X. *Science* **2008**, *321*, 930−930.

(11) Thompson, C. V. *Annu. Rev. Mater. Res.* **2012**, *42*, 399−434.

(12) Hong, S.; Kang, T.; Choi, D.; Choi, Y.; Lee, L. P. *ACS Nano* **2012**, *6*, 5803−5808.

(13) Kim, J. H.; Woo, H. J.; Kim, C. K.; Yoon, C. S. *Nanotechnology* **2009**, *20*, 235306.

(14) Peng, K.-Q.; Wang, X.; Wu, X.-L.; Lee, S.-T. *Nano Lett.* **2009**, *9*, 3704−3709.

(15) Yoo, Y.; Yoon, I.; Lee, H.; Ahn, J.; Ahn, J.-P.; Kim, B. *ACS Nano* **2010**, *4*, 2919−2927.

(16) Gilroy, K. D.; Farzinpour, P.; Sundar, A.; Tan, T.; Hughes, R. A.; Neretina, S. *Nano Res.* **2013**, *6*, 418−428.

(17) Song, C.; Abell, J. L.; He, Y.; Murph, S. H.; Cui, Y.; Zhao, Y. *J. Mater. Chem.* **2012**, *22*, 1150−1159.

(18) Sundar, A.; Hughes, R. A.; Farzinpour, P.; Gilroy, K. D.; Devenyi, G. A.; Preston, J. S.; Neretina, S. *Appl. Phys. Lett.* **2012**, *100*, 013111.

(19) Farzinpour, P.; Sundar, A.; Gilroy, K. D.; Eskin, Z. E.; Hughes, R. A.; Neretina, S. *Nanoscale* **2013**, *5*, 1929−1938.

(20) Henry, C. R. *Prog. Surf. Sci.* **2005**, *80*, 92−116.

(21) Katz, G. *Appl. Phys. Lett.* **1968**, *12*, 161−163.

(22) Farzinpour, P.; Sundar, A.; Gilroy, K. D.; Eskin, Z. E.; Hughes, R. A.; Neretina, S. *Nanotechnology* **2012**, *23*, 495604.

(23) Ma, D. L.; Chen, H. L. *J. Cryst. Growth* **2011**, *335*, 127−132.

(24) Meng, G.; Yanagida, T.; Kanai, M.; Suzuki, M.; Nagashima, K.; Xu, B.; Zhuge, F.; Klamchuen, A.; He, Y.; Rahong, S.; Kai, S.; Kawai, T. *Phys. Rev. E* **2013**, *87*, 012405.

(25) Silly, F.; Castell, M. R. *Phys. Rev. Lett.* **2005**, *94*, 046103.

(26) Kishore, S.; Nelson, J. A.; Adair, J. H.; Eklund, P. C. *J. Alloys Compd.* **2005**, *389*, 234−242.

(27) Langhammer, C.; Yuan, Z.; Zorić, I.; Kasemo, B. *Nano Lett.* **2006**, *6*, 833−838.

(28) Cheong, S.; Watt, J. D.; Tilley, R. D. *Nanoscale* **2010**, *2*, 2045−2053.

(29) Langhammer, C.; Zorić, I.; Kasemo, B. *Nano Lett.* **2007**, *7*, 3122−3127.

(30) Komanicky, V.; Iddir, H.; Chang, K.-C.; Menzel, A.; Karapetrov, G.; Hennessy, D.; Zapol, P.; You, H. *J. Am. Chem. Soc.* **2009**, *131*, 5732−5733.

(31) Yoo, Y.; Seo, K.; Han, S.; Varadwaj, K. S. K.; Kim, H. Y.; Ryu, J. H.; Lee, H. M.; Ahn, J.-P.; Ihee, H.; Kim, B. *Nano Lett.* **2010**, *10*, 432−438.

(32) Heun, S.; Radha, B.; Ercolani, D.; Kulkarni, G. U.; Rossi, F.; Grillo, V.; Salviati, G.; Beltram, F.; Sorba, L. *Cryst. Growth Des.* **2010**, *10*, 4197−4202.

(33) Humphrey, D. S.; Cabailh, G.; Pang, C. L.; Muryn, C. A.; Cavill, S. A.; Marchetto, H.; Potenza, A.; Dhesi, S. S.; Thornton, G. *Nano Lett.* **2009**, *9*, 155−159.

(34) Hofmann, S.; Sharma, R.; Wirth, C. T.; Cervantes-Sodi, F.; Ducati, C.; Kasama, T.; Dunin-Borkowski, R. E.; Drucker, J.; Bennett, P.; Robertson, J. *Nat. Mater.* **2008**, *7*, 372−375.